Andean Geology 36 (2): 153-171. July, 2009

Andean Geology
formerly Revista Geológica de Chile
www.scielo.cl/andgeol.htm

Fission track thermochronology of Neogene plutons in the Principal Andean Cordillera of central Chile (33-35°S): Implications for tectonic evolution and porphyry Cu-Mo mineralization

Víctor Maksaev[1], Francisco Munizaga[1], Marcos Zentilli[2], Reynaldo Charrier[1]

[1] *Departamento de Geología, Universidad de Chile, Casilla 13518, Correo 21, Santiago, Chile. vmaksaev@ing.uchile.cl; fmunizag@cec.uchile.cl; rcharrie@cec.uchile.cl*
[2] *Department of Earth Sciences, Dalhousie University, Halifax, Nova Scotia, Canada B3H 4J1 marcos.zentilli@dal.ca*

ABSTRACT. Apatite fission track data for Miocene plutons of the western slope of the Principal Andean Cordillera in central Chile (33-35°S) define a distinct episode of enhanced crustal cooling through the temperature range of the apatite partial annealing zone (~125-60°C) from about 6 to 3 Ma. This cooling episode is compatible with accelerated exhumation of the plutons at the time of Pliocene compressive tectonism, and mass wasting on the western slope of the Principal Andean Cordillera in central Chile. The timing coincides with the southward migration of the subducting Juan Fernández Ridge and the development of progressive subduction flattening northward of 33°S. It also corresponds to the time of active magmatic-hydrothermal processes and rapid unroofing of the world class Río Blanco-Los Bronces and El Teniente porphyry Cu-Mo deposits. Zircon fission track ages coincide with previous $^{40}Ar/^{39}Ar$ dates of the intrusions, and with some of the apatite fission track ages, being coherent with igneous-linked, rapid cooling following magmatic intrusion. The thermochronologic data are consistent with a maximum of about 8 km for Neogene exhumation of the plutons.

Keywords: Thermochronology, Andes, Fission track, Apatite, Porphyry copper, Exhumation.

RESUMEN. Termocronología mediante trazas de fisión de plutones neógenos en la Cordillera Principal Andina de Chile central (33-35°S): Implicancias para la evolución tectónica y mineralización de pórfidos de Cu-Mo. Los datos de trazas de fisión en apatita de plutones miocenos del flanco oeste de la Cordillera Principal de Chile central (33-35°S) definen un episodio distintivo de enfriamiento acelerado a través del rango de temperatura de la zona de acortamiento parcial de trazas en apatita (~125-60°C) entre los 6 a 3 Ma. Este episodio de enfriamiento es compatible con exhumación rápida de los plutones al tiempo del tectonismo compresivo plioceno y remociones en masa en el flanco oeste de la Cordillera Principal en Chile central. El período de tiempo coincide con la migración hacia el sur de la subducción de la Dorsal de Juan Fernández y con el desarrollo de un aplanamiento progresivo de la subducción hacia el norte de los 33°S. También corresponde al tiempo de actividad magmático-hidrotermal y rápido desenterramiento de los pórfidos de Cu-Mo de clase mundial de Río Blanco-Los Bronces y El Teniente. Las edades de circones por trazas de fisión coinciden con datos geocronológicos $^{40}Ar/^{39}Ar$ previos a las intrusiones y con algunas de las edades de trazas de fisión en apatitas, siendo coherentes con el enfriamiento rápido relacionado con procesos ígneos después de la intrusión magmática. Los datos son consistentes con un máximo de aproximadamente 8 km para la exhumación neógena de los plutones.

Palabras claves: Termocronología, Andes, Trazas de fisión, Apatita, Pórfido cuprífero, Exhumación.

1. Introduction

The subduction-related Miocene-Pliocene volcanism and plutonism along the Principal Andean Cordillera of central Chile (33-35°S) developed synchronously with crustal thickening and tectonic uplift related to compressive tectonism (Miocene Quechua, and Pliocene Diaguita phases, described originally by Steinmann (1929) in Perú and by Salfity *et al*. (1984) in northwestern Argentina; see also the review of González-Bonorino *et al*., 2001). This Andean segment occurs immediately southeast of the place where the Juan Fernández Ridge is being subducted (Fig. 1), which has migrated from north to south during the Late Cenozoic (Yáñez *et al*., 2001, 2002). The progressive decrease in the angle of subduction of Nazca oceanic lithosphere northward from 33°S has been attributed to the Juan Fernández Ridge subduction (Yáñez *et al*., 2001, 2002). Crustal deformation resulting in increased crustal thickness and possibly dehydration and/or melting of thickened lower continental crust have also been credited to the effects of the ridge subduction (Kay *et al*., 1999, 2005; Kay and Mpodozis, 2002), and higher exhumation rates during the Neogene (Skewes and Holmgren, 1993; Kurtz *et al*., 1997). In addition, the giant porphyry Cu-Mo deposits of Río Blanco-Los Bronces and El Teniente (Fig. 1) were formed in this Andean segment during the late Miocene to early Pliocene (Deckart *et al*., 2005, 2006; Maksaev *et al*., 2004; Cannell *et al*., 2005) and were rapidly unroofed (Skewes and Holmgren, 1993; Serrano *et al*., 1996). Their origin has been attributed to crustal thickening, uplift and erosion that accelerated crystallization and devolatilization of crustal magma chambers above which the giant Cu-Mo deposits were formed (Skewes and Stern, 1994; Stern and Skewes, 2005). Thus, understanding the Neogene exhumation history of the Principal Andean Cordillera of central Chile has implications for both the tectonic and metallogenic evolution of this segment of the Andean orogen.

A number of plutons of the Principal Andean Cordillera of central Chile were previously dated by the $^{40}Ar/^{39}Ar$ method by Kurtz *et al*. (1997). These authors modelled the exhumation of two Miocene plutons (La Obra and Nacimiento Cortaderal) based on differences of biotite and K-feldspar plateau $^{40}Ar/^{39}Ar$ ages that were ascribed to unverified exhumation-linked cooling. We have analyzed zircon and apatite crystals from the same Miocene intrusive bodies by fission track thermochronology (Fig. 2; Table 1), establishing their low temperature cooling histories with the goal to improve the understanding of the exhumation history of the western slope of the Principal Andean Cordillera in central Chile, as a contribution to constrain the tectonic and metallogenic evolution of this Andean segment. Analyses were done on some of the remaining samples from the 'Proyecto Geodinámico El Teniente' of CODELCO-Chile, which were originally dated by Kurtz *et al*. (1997), plus additional samples collected specifically for this study. The extended geographical spread of the samples in the region (Fig. 2; Table 1) allows assessment of variations of the cooling histories of the plutons. The fission track low-temperature thermochronology is evaluated relative to the published geochronological data of the Miocene plutons to constrain their time-temperature history and the implications of the new data for tectonics and metallogeny are discussed.

2. Geological Framework

The segment of the Andes between 33° and 35°S is situated immediately south of the flat-slab segment of the subducted oceanic Nazca Plate (28-33°S; Cahill & Isacks, 1992; Yáñez *et al*., 2002). Thus the subducting Nazca slab sharply flexes southwards from subhorizontal to a dip angle 25-30° (Pardo *et al*., 2002). The rough mountainous western flank of the Principal Andean Cordillera in central Chile is about 60 km wide, varying from about 1,000 m up to 6,969 m above sea level (Mount Aconcagua; Fig. 1). Most of the highest peaks are Andean arc volcanoes of the currently active Southern Volcanic Zone, which extends from 33°S southward along the continental watershed (*e.g.,* 6,570 m at the summit of the Tupungato volcano). A Miocene-Pliocene fold-thrust belt and a foreland basin system extends farther east into Argentinean territory (Fig. 1), and a 50 km wide alluvial plain (the Central Depression; Fig. 2) borders the Principal Andean Cordillera to the west; the plain slopes westward from about 700 down to 400 m, where it adjoins the Coastal Cordillera (Fig. 2).

Oligocene-Miocene volcanic successions, totaling about 2,600 to 4,900 m in thickness, are exposed on most of the western flank of the Principal Andean Cordillera in central Chile. Traditionally the 1,300 to 1,900 m thick, folded lower section (Oligocene to early Miocene in age) has been mapped as the

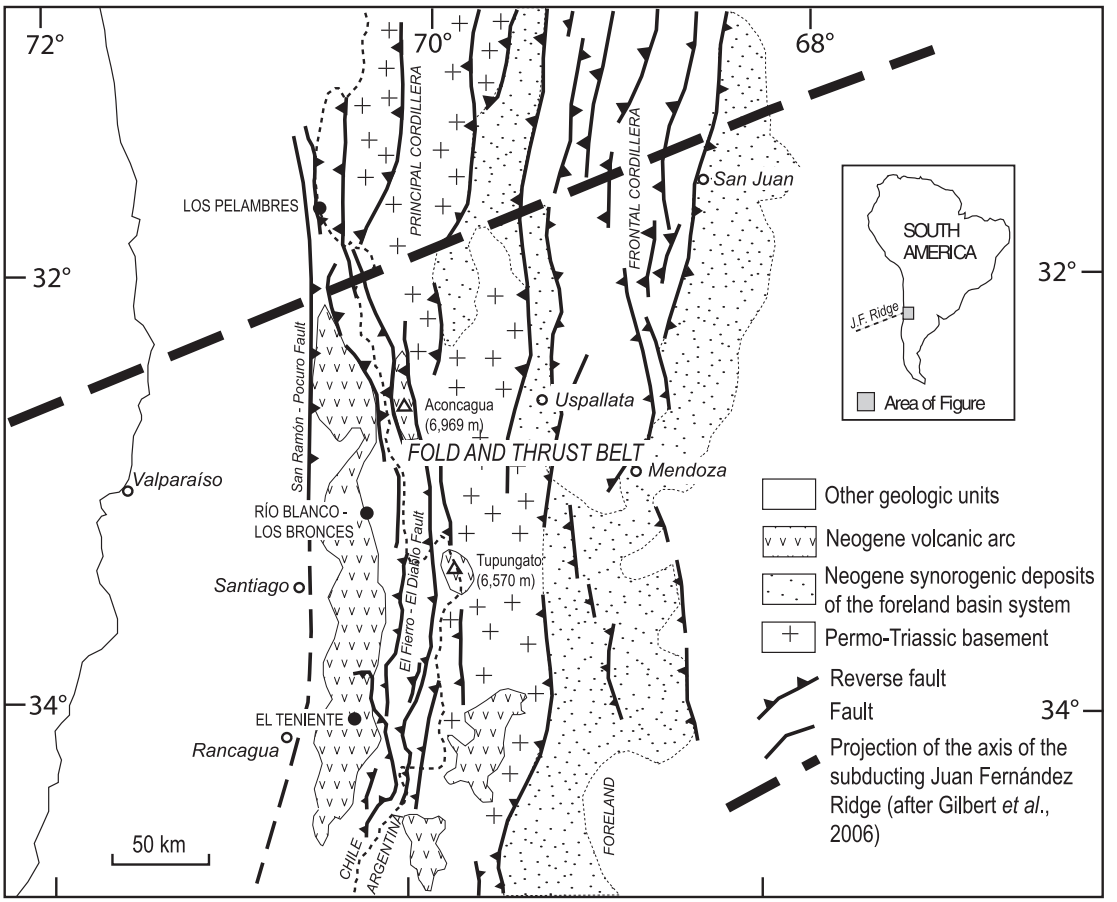

FIG. 1. Structural setting of the Principal Cordillera of the Andes in central Chile and western Argentina, showing the main faults of the Aconcagua fold and thrust belt, synorogenic clastic sedimentary deposits in the foreland basin system in Argentina, and the projection of the axis of the subducting Juan Fernández Ridge under the orogen. Figure modified after Sillitoe and Perelló (2005) with fold and thrust belt and synorogenic deposits from Ramos *et al*. (1996) and faults in Chile from Farías *et al*. (2008); the projection of the axis of the Juan Fernández Ridge after Gilbert *et al*. (2006).

Abanico Formation or the equivalent Coya-Machalí Formation south of 34°S (Klohn, 1960; Aguirre, 1960; Thiele, 1980; Charrier *et al*., 2002, 2005), whereas the upper unconformable subhorizontal volcanic rocks (1,300 to 3,000 m thick) are considered to be part of the Farellones Formation (Charrier *et al*., 2002). In fact, a progressive unconformity (time-transgressive) separates these units and the K-Ar ages of the two volcanic units overlap between 22 and 16 Ma (Nyström *et al*., 2003; Charrier *et al*., 2002, 2005, 2007). The volcanism of the Principal Andean Cordillera of central Chile appears to have initially developed during the Eocene-Oligocene under an extensional tectonic regime (Charrier *et al*., 2002). However, during the Miocene, volcanic activity took place simultaneously with compressive pulses of the Quechua tectonic phase and related crustal shortening. Subsequently, volcanic activity practically waned, and only very localized igneous activity was recorded in the region during the Pliocene Diaguita compressive tectonic phase (*e.g.*, González-Bonorino *et al*., 2001). The igneous activity completely ceased by the late Pliocene along the western flank of the Principal Andean Cordillera, except for the currently active Southern Volcanic Zone of the Andes, which developed since the latest Pliocene farther east along the continental watershed. Basin inversion and significant tectonic uplift of the Principal Andean Cordillera took place as a result of the Neogene compressive tectonism

TABLE 1. SAMPLE LOCATIONS.

Sample	Unit	Lithology	Latitude S	Longitude W	Altitude (m)
TT-127	San Francisco	granodiorite	33°04'56.7"	70°15'18.9"	2,740
TT-128	San Francisco	granodiorite	33°05'44.0"	70°15'17.0"	2,910
TT-190	Río Blanco	granodiorite	33°07'15.0"	70°14'50.0"	3,245*
TT-188	Río Blanco	granodiorite	33°08'23.6"	70°16'04.0"	2,784*
TT-189	Río Blanco	granodiorite	33°08'39.6"	70°15'12.0"	2,616*
TT-115	La Obra	granodiorite	33°35'40.8"	70°29'23.2"	760
TT-118	San Gabriel	granodiorite	33°47'33.1"	70°12'32.5"	1,370
ETP-4	San Gabriel	granodiorite	33°48'37.4"	70°12'34.2"	1,315
ETP-3	San Gabriel	quartz monzodiorite	33°49'29.1"	70°12'53.4"	1,560
ETP-11	Jeria	diorite	34°00'35.5"	70°01'11.8"	2,700
ETP-12	Extravío	quartz monzodiorite	34°02'34.7"	70°16'29.4"	3,030
ETP-10A	Alfalfalito	quartz monzodiorite	34°05'12.7"	70°07'07.4"	2,650
ETP-14	Cruz de Piedra	quartz monzodiorite	34°12'10.3"	69°55'36.6"	3,790
ETP-13	Río Pangal	quartz monzonite	34°14'17.3"	70°19'21.7"	1,490
ETP-8A	Estero Crucero	granodiorite	34°26'31.7"	70°08'06.7"	3,150
ETP-8B	Estero Crucero	quartz monzodiorite	34°26'31.7"	70°08'06.7"	3,150
ETP-17	Rosario de Rengo	quartz monzodiorite	34°33'28.7"	70°32'32.7"	1,830
ETP-7	Río Cortaderal	granodiorite	34°35'46.1"	70°14'26.7"	2,680

* Underground samples

(Godoy *et al*., 1999; Charrier *et al*., 2002, 2005), but also the synchronous development of a foreland basin system farther east in Argentina (Giambiagi *et al*., 2001).

A number of Miocene granodioritic to dioritic plutons are scattered throughout the Cordillera at these latitudes (*e.g.*, Kurtz *et al*., 1997); some of them are composite intrusions and locally display sill geometry within the Oligocene-Miocene volcanic succession. In addition, this segment of the Andes encompasses two of the largest porphyry Cu-Mo deposits in the world, the Río Blanco-Los Bronces and El Teniente. These deposits occur within hydrothermal alteration zones related to late Miocene-early Pliocene multiphase porphyritic stocks (Skewes *et al*., 2002; Maksaev *et al*., 2004; Deckart *et al*., 2005, 2006) (Figs. 1 and 2). The waning stage of Pliocene arc-related igneous activity and the formation of giant Cu-Mo deposits preceded a 50 km eastward arc migration, to the currently active Southern Volcanic Zone of the Andes (Kay *et al*., 2005).

Remnants of Pliocene rock debris (avalanche deposits) occur scattered along the westernmost section of the Principal Andean Cordillera between 33° and 34°S in central Chile (*e.g.*, SERNAGEOMIN, 2002) and within sections of the Central Depression (Marangunic *et al*., 1979). The Pliocene rock debris records massive landslides of upper Miocene volcanic materials from the Principal Andean Cordillera (*e.g*., Encinas *et al*., 2006).

3. Fission Track Thermochronology

Zircon and apatite fission track analysis are methods that provide quantitative information on the thermal histories of rocks (*e.g.*, Gallagher *et al*., 1998). The temperatures at which fossil fission tracks within the apatite and zircon mineral groups partially anneal (*i.e.*, partial age resetting) are not sharply defined but progressive (Green *et al*., 1986). The temperature range where partial track annealing occurs is known to be a function of the phase composition (Green *et al*., 1986; Carlson *et al*., 1999), cooling rate, and possibly the symmetry group of the mineral (Spikings *et al*., 2005 and references therein).

Unannealed track lengths in apatite range between *ca*. 14.5 and 15.5 μm relative to standard Durango apatite (Gleadow *et al*., 1986), and hence apatite samples that have mean track lengths in this range, combined with narrow track length distributions, have experienced rapid monotonic cooling from temperatures of ≥125-100°C to temperatures

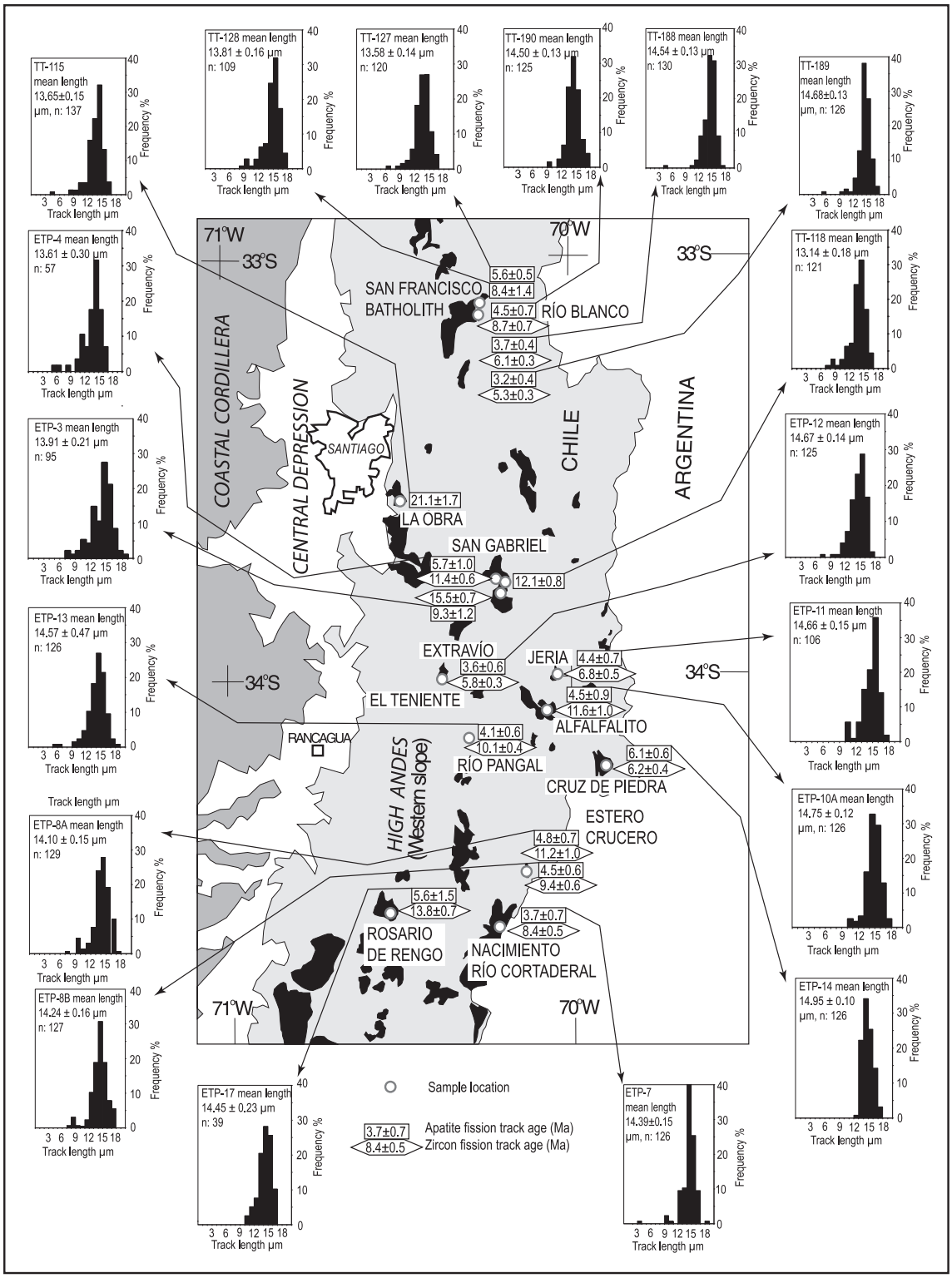

FIG. 2. Zircon and apatite fission track ages, and confined apatite track length distributions for Miocene plutons (black colored) in the western slope of the Principal Andean Cordillera of central Chile.

of *ca.* ≤60°C at the time indicated by the respective apatite fission track age (Laslett *et al*., 1987). Broad track length distributions with shorter mean lengths reveal instead that the sample experienced a more complex thermal history, spending a significant amount of time within the partial annealing zone (Gleadow *et al*., 1986; Spikings *et al*., 2005). Similar principles apply to zircon fission track data, but the lack of well-characterized annealing kinetics of tracks within zircon precludes the determination of a thermal history from the track length distributions. In most geological settings zircon has an effective closure temperature of about 240±50°C (Hurford, 1986; Brandon *et al*., 1998; Bernet *et al.*, 2002). However, experimental data show that there is a wide temperature range, from 160 to 380°C, for the temperature bounds for the zircon partial annealing zone, which are strongly dependent on cooling rates and alpha radiation damage of zircon crystals (Bernet and Garver, 2005; Tagami, 2005; Reiners and Brandon, 2006). Thus, as a reasonable approximation for this work, a temperature of 280±30°C has been plotted against the zircon fission track age in study to produce a single temperature-time point on a thermal history path (*e.g.*, Tagami and Shimada, 1996; Thomson *et al*., 2001; Reiners and Brandon, 2006; Adriasola and Stökhert, 2008).

4. Analytical Methods

Apatite and zircon were separated by conventional methods at the facilities of the Universidad de Chile. The zircon and most of apatite fission track analyses were done by Dr. P.B. O'Sullivan in the 'Apatite to Zircon, Inc.' Laboratory, Idaho, USA, and some of the apatite fission track analyses were done by A.M. Grist at the Fission Track Laboratory of Dalhousie University, Halifax, Nova Scotia, Canada. Etching of natural fission tracks in apatite was attained by immersion in 5.5N HNO_3 for 20.0 seconds (±0.5 seconds), whereas etching of zircon grains was done by immersion in an eutectic melt of NaOH+KOH at 210°C (±10°C). Total etching times for zircons varied between 25 and 69 hours, but for most samples was 44 hours and 15 minutes. The external detector method was used for fission track dating (Gleadow, 1981), ages were calculated using the zeta calibration method (Hurford and Green, 1983), and errors were calculated according to conventional methods (Green, 1981). Analyses done at the 'Apatite and Zircon, Inc.' included the systematic measurement of the maximum fission track etch pit diameters oriented within 5° of the c axis of the apatite crystal (Dpar) in order to consider fission-track annealing variability among different apatite species in thermal history modelling (Carlson *et al*., 1999). Irradiation of apatite samples with ^{252}Cf was used to increase the amount of etched confined track for length measurement. The precision of each track length is estimated to be ±0.20 μm.

The AFTsolve multi-kinetic inverse modelling program of apatite fission track data (Ketcham *et al*., 2000) was used to derive time-temperature histories from the fission track data of apatite samples. This program implements various laboratory calibrations of the behaviour of fission tracks in apatite in response to heating and cooling histories, and calculates the range of thermal histories that are potentially consistent with the measured age and the measured frequency distribution of confined track lengths. Full details concerning these calibrations and the various uses of AFTsolve are publicly available (Carlson *et al*., 1999; Donelick *et al*., 1999; Ketcham *et al*., 1999, 2000). 20,000 random time-temperature paths are created by a Monte Carlo scheme, and for each path the resulting fission track age and track length distribution are calculated, and the goodness-of-fit between calculated and measured data is evaluated by a Kolmogorov-Smirnov test. The program maps out the time-temperature regions that envelop all thermal histories with 'good' and 'acceptable' fit, corresponding to goodness-of-fit values from 0.5 to 1 and from 0.05 to 0.5, respectively.

5. Results and discussion

Apatite fission track ages from 3.2±0.7 to 21.1±3.4 Ma were obtained for eighteen samples from Miocene plutons that are spread on the western slope of the Principal Andean Cordillera of central Chile (33-35°S) and span elevations between 760 and 3,790 m (Table 2; Fig. 2). In addition, 14 zircon fission track ages, which range between 5.3±0.3 and 13.8±0.7 Ma (Table 3; Fig. 2), were obtained for the same plutons.

Most of the zircon fission track ages are similar to their respective biotite $^{40}Ar/^{39}Ar$ or K-Ar ages, except for the Extravío pluton with a zircon fission track ~1 m.yrs. younger than a biotite $^{40}Ar/^{39}Ar$ age (Table 4), but in this case the ages are for separate

TABLE 2. APATITE FISSION TRACK ANALYTICAL DATA.

Sample	Pluton	N°G	ρ_s (10^6 tracks/ cm^2)	N_s (tracks)	ρ_i (10^6 tracks/ cm^2)	N_i (tracks)	ρ_d (10^6 tracks/ cm^2)	N_d (tracks)	$p>\chi^2$	Apatite FT Age (Ma±1σ)	Mean length ± S.E. (μm±1σ)	S.D. (μm)	N° tlm	Dpar (μm)
TT-127	San Francisco	22	0.072	114	2.756	4,370	1.21	5,405	0.786	5.6±0.5	13.58±0.14	1.57	120	-
TT-128	San Francisco	10	0.092	38	2.11	876	1.10	4,916	0.982	8.4±1.4	13.81±0.16	1.69	109	-
TT-190	Río Blanco	25	0.051	47	1.977	1,819	3.359	4,279	0.996	4.5±0.7	14.50±0.13	1.42	125	2.83
TT-188	Río Blanco	25	0.102	89	4.897	4,254	3.400	4,279	0.263	3.7±0.4	14.54±0.13	1.53	130	1.63
TT-189	Río Blanco	25	0.073	79	4.100	4,430	3.380	4,279	0.494	3.2±0.4	14.68± 0.13	1.50	126	1.65
TT-115	La Obra	18	0.345	175	3.49	1,771	1.21	5,405	0.553	21.1±1.7	13.65±0.15	1.73	137	-
TT-118	San Gabriel	26	0.158	286	2.789	5,034	1.21	5,405	0.966	12.1±0.8	13.14±0.18	1.99	121	-
ETP-4	San Gabriel	25	0.052	49	2.150	2,016	3.299	4,279	0.039	5.7±1.0	13.61±0.30	2.23	57	2.16
ETP-3	San Gabriel	28	0.061	64	1.143	1,190	3.319	4,279	0.927	9.3±1.2	13.91±0.21	2.07	95	2.64
ETP-11	Jeria	25	0.067	42	2.545	1,586	3.197	4,279	0.866	4.4±0.7	14.66±0.15	1.54	106	2.71
ETP-12	Extravío	25	0.038	37	1.752	1,719	3.177	4,279	0.880	3.6±0.6	14.67±0.14	1.60	125	2.57
ETP-10A	Alfalfalito	25	0.031	28	1.152	1,047	3.218	4,279	0.919	4.5±0.9	14.75±0.12	1.30	126	2.08
ETP-14	Cruz de Piedra	25	0.131	116	3.520	3,109	3.137	4,279	0.188	6.1±0.6	14.95±0.10	1.07	126	3.34
ETP-13	Río Pangal	25	0.047	45	1.912	1,817	3.157	4,279	0.714	4.1±0.6	14.57±0.47	5.27	126	1.98
ETP-8A	Estero Crucero	25	0.046	45	1.635	1,601	3.258	4,279	0.205	4.8±0.7	14.10±0.15	1.75	129	1.78
ETP-8B	Estero Crucero	25	0.072	52	2.706	1,957	3.238	4,279	0.801	4.5±0.6	14.24±0.16	1.81	127	2.40
ETP-17	R. de Rengo	14	0.033	14	0.952	410	3.116	4,279	0.964	5.6±1.5	14.45±0.23	1.41	39	1.93
ETP-7	Río Cortaderal	25	0.044	34	2.046	1,571	3.278	4,279	0.689	3.7±0.7	14.39±0.15	1.68	126	2.01

Analyses by Dr. Paul B. O'Sullivan of Apatite to Zircon Inc., Viola, Idaho, U.S.A. (N_d = 4,279) and by Dr. Alexander M. Grist at the Fission Track Laboratory of Dalhousie University (N_d= 5,405). A value of 104.5±2.6 (CN-1) was used for the zeta calibration factor at Apatite to Zircon Inc. and of 353.5±7.1 (CN-5) at Dalhousie University.
Samples with $p>\chi^2$ greater than 0.05 pass the χ^2 test at 95% confidence level (*i.e.*, appear to be composed of one age population). Ages reported for these samples are calculated using pooled statistics. Ages reported for samples which fail the χ^2 test are the central age (Galbraith and Laslett, 1993). Abbreviations are as follows: ρ_s, ρ_i, and ρ_d, wich are the density of spontaneous, induced, and flux dosimeter tracks, respectively (x10^6/cm^2). N_s, N_i and N_d. are the number of spontaneous, induced, and glass dosimeter (CN-5 or CN-1) tracks, respectively. **N°G.** is the number of individual grains dated; **S.E.** is the standard error; **S.D.** is the standard deviation; **N°tlm.** is the number of measured track length; **Dpar.** is the maximum fission track etch pit diameter oriented within 5° of the c axis of the apatite grain.

TABLE 3. ZIRCON FISSION TRACK ANALYTICAL DATA.

Sample	Pluton	Grains	ρ_s (10^6 tracks/cm^2)	N_s (tracks)	ρ_i (10^6 tracks/cm^2)	N_i (tracks)	ρ_d (10^6 tracks/cm^2)	N_d (tracks)	$p>\chi^2$	Zircon FT Age (Ma±1σ)
TT-190	Río Blanco	25	0.883	569	4.554	2,935	0.671	4,030	0.000	8.7±0.7
TT-188	Río Blanco	25	2.093	1,039	14.348	7,124	0.673	4,030	0.325	6.1±0.3
TT-189	Río Blanco	25	0.729	774	5.759	6,116	0.672	4,030	0.025	5.3±0.3
ETP-3	San Gabriel	20	5.478	4,839	14.815	13,087	0.669	4,030	0.000	15.5±0.7
ETP-4	San Gabriel	25	1.574	842	5.753	3,077	0.668	4,030	0.394	11.4±0.6
ETP-11	Jeria	25	1.047	758	6.692	4,846	0.664	4,030	0.000	6.8±0.5
ETP-12	Extravío	25	3.414	1,231	24.220	8,734	0.663	4,030	0.998	5.8±0.3
ETP-10A	Alfalfalito	23	1.243	1,029	4.658	3,857	0.664	4,030	0.000	11.6±1.0
ETP-14	Cruz de Piedra	20	0.786	440	5.209	2,915	0.661	4,030	0.262	6.2±0.4
ETP-13	Río Pangal	25	3.039	2,019	12.459	8,278	0.662	4,030	0.055	10.1±0.4
ETP-8A	Estero Crucero	22	1.710	1,014	6.510	3,861	0.666	4,030	0.000	11.2±1.0
ETP-8B	Estero Crucero	20	2.886	2,549	13.271	11,723	0.665	4,030	0.000	9.4±0.6
ETP-17	Rosario de Rengo	25	0.802	684	2.391	2,040	0.660	4,030	0.985	13.8±0.7
ETP-7	Río Cortaderal	25	1.836	1,146	9.478	5,916	0.667	4,030	0.010	8.4±0.5

Analyses by Dr. Paul B. O'Sullivan at Apatite to Zircon Inc., Viola, Idaho, U.S.A. A value of 124.7±3.2 (CN-1) was used for the zeta calibration Samples with $p>\chi^2$ greater than 0.05 pass the χ^2 test at 95% confidence level. Ages reported for these samples are calculated using pooled statistics. Ages reported for samples which fail the χ^2 test are the central age (Galbraith and Laslett, 1993). Abbreviations are as follows: ρ_s, ρ_i, and ρ_d, wich are the density of spontaneous, induced, and flux dosimeter tracks, respectively (x10^6/cm^2). N_s, N_i, and N_d are the number of spontaneous, induced, and dosimeter (CN5 or CN1) tracks, respectively.

samples 4.5 km apart, respectively. The 13.8±0.7 Ma zircon fission track for the Rosario de Rengo pluton appears to be younger than the respective hornblende $^{40}Ar/^{39}Ar$ of 16.2±1.3 Ma, but these dates overlap at ±2σ error limits. On the other hand, the samples from the Río Blanco granodiorite yielded zircon fission track ages between 8.7±0.7 and 5.3±0.3 Ma, which are significantly younger than the 11.96±0.40 Ma zircon U-Pb age of their host rock (Table 4). These samples were obtained from drill cores within the Río Blanco porphyry copper deposit (TT-188, TT-189) and its surroundings (TT-190), where the thermal history is complicated by a succession of younger intrusions that are associated with porphyry copper mineralization and hydrothermal alteration (*e.g.*, Deckart *et al*., 2005). In fact, the zircon fission track ages for the Río Blanco granodiorite coincide with zircon U-Pb ages of other younger intrusive bodies emplaced within this intrusion at the Río Blanco porphyry copper deposit area (the Cascada Granodiorite, Quartz Monzonite, and Don Luis Porphyry; Table 4). Consequently thermal aureoles of other intrusions might have reset the zircon fission track system of the Río Blanco granodiorite at the homonymous porphyry copper deposit. As a reference, Tagami and Shimada (1996) have shown that zircon fission track ages in sandstones surrounding a rapidly cooled granitic intrusion become totally reset within a distance of ~3 km from a steep-dipping contact, although this distance can vary depending on several factors, including the size and shape of the intrusives, the permeability of the wallrock, the depth of emplacement, and the presence of fluids (*e.g.*, Adriasola *et al*., 2006).

The zircon fission track ages are interpreted to represent the time of post-emplacement cooling to temperatures of around 280±30°C (*e.g.*, Tagami and Shimada, 1996; Bernet and Garver, 2005; Reiners and Brandon, 2006), and the biotite $^{40}Ar/^{39}Ar$ closure temperature can be estimated as 320±30°C using Dodson (1973) and parameters presented by Harrison *et al*. (1985) and McDougall and Harrison (1999). Therefore, the overall coincidence of the zircon fission track ages with biotite $^{40}Ar/^{39}Ar$ ages (Table 4) is consistent with *in situ* post-magmatic rapid cooling of the host intrusions. The dated plutons should have remained at a cool (shallow) level in the crust since their emplacement, where temperatures have not been high enough to significantly anneal the fission tracks in the zircon grains (within the zircon fission track retention zone); except for subsequent heat input from other intrusions that may have lead to annealing of zircon fission tracks at Río Blanco. Therefore Neogene exhumation has not been sufficient to expose Miocene intrusive rocks from depths corresponding

to the zircon partial annealing zone. The lower temperature bound of the zircon partial annealing zone may be as high as 250°C for non damaged zircons and rapid cooling rates (Tagami, 2005; Reiners and Brandon, 2006), implying that the Neogene exhumation has been limited to a column of less than ~8 km, assuming a paleogeothermal gradient of 30°C/km. This establishes a maximum for the Neogene exhumation in this part of the Andes that is consistent with the preservation of a succession of more than 3,000 m of Oligocene-Miocene volcanic rocks along the western slope of the Principal Cordillera of central Chile.

The above geothermal gradient is speculative, but not unreasonable as a first approximation, since Giese (1994), on the basis of thermal measurements and calculations for the present-day crust in the Central Andes, estimates a temperature of 141°C at a depth of 5 km (average gradient of 28.2°C/km), and regional surface heat flow measurements yield current values of ~80-100 mW/m^2 (Hamza and Muñoz, 1996; Muñoz, 1999). Thermal conductivities for granitoids vary between 2.5 and 3.5 W/(m°K) (Seipold, 1998). Thus, present-day geothermal gradients of 32±8°C/km can be estimated for the upper crust (Adriasola *et al*., 2006); if a higher geothermal gradient was prevalent during the Neogene arc magmatism it would signify even less exhumation.

The apatite fission track ages obtained for the La Obra, San Gabriel and Cruz de Piedra plutons are similar to zircon fission track ages and/or previous $^{40}Ar/^{39}Ar$ or K-Ar ages of the respective intrusions (Table 4). However, most of the apatite fission track ages are 2 to 7 m.yrs. younger than their respective

TABLE 4. ZIRCON AND APATITE FISSION TRACK AGES COMPARED TO PREVIOUS GEOCHRONOLOGICAL DATA.

Sample	Pluton	Apatite FT Age (Ma±1σ)	Zircon FT Age (Ma±1σ)	Age	Previous radiometric dates Mineral and method (reference)
TT-127	San Francisco	5.6±0.5	-	14.6±0.5	Biotite K-Ar (1)
TT-190	Río Blanco Granodiorite*	4.5±0.7	8.7±0.7	11.96±0.40 8.40±0.23	Zircon U-Pb (2) Zircon U-Pb Cascada granodiorite (2)
TT-188	Río Blanco Granodiorite*	3.7±0.4	6.1±0.3	11.96±0.40 6.32±0.09	Zircon U-Pb (2) Zircon U-Pb Quartz monzonite (2)
TT-189	Río Blanco Granodiorite*	3.2±0.4	5.3±0.3	11.96±0.40 5.23±0.07	Zircon U-Pb (2) Zircon U-Pb Don Luis porphyry (2)
TT-115	La Obra	21.1±1.7	-	21.6±2.5	Hornblende $^{40}Ar/^{39}Ar$ (3)
TT-118	San Gabriel	12.1±0.8	-	11.5±0.1	Biotite $^{40}Ar/^{39}Ar$ (3)
ETP-3	San Gabriel	9.3±1.2	15.5±0.7	13.6±0.8	Biotite K-Ar (4)
ETP-4	San Gabriel	5.7±1.0	11.4±0.6	11.3±0.3	Biotite $^{40}Ar/^{39}Ar$ (3)
ETP-7	Nacimiento Río Cortaderal	3.7±0.7	8.4±0.5	8.4±0.3 7.7±0.1	Biotite $^{40}Ar/^{39}Ar$ (3) K-feldspar $^{40}Ar/^{39}Ar$ (3)
ETP-8A	Estero Crucero	4.8±0.7	11.2±1.0	-	-
ETP-8B	Estero Crucero	4.5±0.6	9.4±0.6	8.8±0.1	Biotite $^{40}Ar/^{39}Ar$ (3)
ETP-10A	Alfalfalito	4.5±0.9	11.6±1.0	12.3±0.2	Biotite $^{40}Ar/^{39}Ar$ (3)
ETP-11	Jeria	4.4±0.7	6.8±0.5	6.6±0.1	Biotite $^{40}Ar/^{39}Ar$ (3)
ETP-12	Extravío	3.6±0.6	5.8±0.3	6.97±0.05	Biotite $^{40}Ar/^{39}Ar$ (5)
ETP-13	Río Pangal	4.1±0.6	10.1±0.4	10.8±0.3	Biotite K-Ar (6)
ETP-14	Cruz de Piedra	6.1±0.6	6.2±0.4	5.5±0.2	Biotite $^{40}Ar/^{39}Ar$ (3)
ETP-17	Rosario de Rengo	5.6±1.5	13.8±0.7	16.2±1.3	Hornblende $^{40}Ar/^{39}Ar$ (3)

References: (1) Rivera and Navarro, 1996[1]; (2) Deckart *et al*., 2005; (3) Kurtz *et al*., 1997; (4) Vergara and Drake, 1978; (5) Maksaev *et al*., 2004; (6) Rivera and Falcón, 1998[2].

* Samples TT-188, TT-189, and TT-190 are from the Río Blanco Granodiorite of the San Francisco Batholith, which is intruded by the Cascada granodiorite, and the Quartz monzonite and Don Luis porphyries.

[1] Rivera, O.; Navarro, M.H. 1996. Estudio geológico distrital de la División Andina de Codelco-Chile, 2ª etapa, escala 1:25.000. Corporación Nacional del Cobre (Chile), Gerencia de Exploraciones: 169 p. (unpublished report).

[2] Rivera, O.; Falcón, M.F. 1998. Estudio Geológico Distrital de la División El Teniente de Codelco-Chile, escala 1:25.000. Codelco-Chile/CEG Ltda.: 268 p. (unpublished report).

$^{40}Ar/^{39}Ar$, K-Ar or zircon fission track ages (plutons: Río Blanco, Jeria, Extravío, Alfalfalito, Río Pangal, Estero Crucero, Rosario de Rengo, and Nacimiento Río Cortaderal; Table 4). Their apatite fission track ages fall within the restricted range from 5.6 to 3.2 Ma (Table 4) that represents the period when the host plutons cooled through the temperature range of the apatite partial annealing zone (~125-60°C; Gleadow *et al*., 1986; Green *et al*., 1986; Carlson *et al*., 1999).

The mean length and distribution of confined tracks in apatite provide important additional information on the cooling history below ~125°C (*e.g.*, Gleadow *et al*., 1986; Green *et al*., 1989). In general, the measured apatite fission track length distributions have long mean track lengths (>14.0 μm) and standard deviations under 1.8 μm (apatite samples from Río Blanco, Extravío, Alfalfalito, Cruz de Piedra, Río Pangal, Estero Crucero, Santa Rosa de Rengo, and Nacientes Río Cortaderal plutons; Fig. 3), indicative of rapid cooling through the temperature range of the apatite partial annealing zone (~125-60°C; Gleadow *et al*., 1986). However, six apatite samples (from San Francisco, La Obra, San Gabriel plutons) have shorter mean track lengths (between 13 and 14 μm) and negative-skewness towards shorter tracks (Fig. 3), which indicate that their host rocks spent some time in the temperature zone where fission tracks in apatite were partially annealed (Gleadow *et al*., 1986). The relationship between the apatite fission track age, and the mean track length and standard deviation for all samples, which yielded adequate length data (Table 2) are plotted in figure 3. The overall 'boomerang' pattern of the plotted fission track data in figure 3 is indicative of partial and total resetting, or exhumation of a fossil partial annealing zone. The long track lengths (>14 μm) and small standard deviations (<1.5 μm) of a group of apatite samples from these plutons and their age data define a distinctive rapid cooling episode between ~6 and 3 Ma; whereas another group of apatite samples displays higher degrees of track shortening (<14 μm) and larger standard deviations (>1.5 μm), thus their apatite fission track data suggest a more complex cooling and/or thermal history.

Figure 4a shows sample apatite fission track ages with track lengths above 14 μm plotted *versus* altitude. Despite scattering, probably due to the extended geographical spread of the samples in this region, there is a general tendency for older apatite fission track ages to correlate with high altitude above sea level, as would be expected for exhumation-related cooling. The same tendency is apparent in the subset of three drill core samples of the Río Blanco granodiorite (Fig. 4b). As a reference, dashed lines corresponding to hypothetical exhumation rates of 0.45 mm/y are shown on figures 4a and 4b, but the actual exhumation rates could have been somewhat higher or lower than this given the errors on the ages. Alternatively, the apatite fission track ages, which are 2 to 7 m.yrs. younger than their respective $^{40}Ar/^{39}Ar$, K-Ar or zircon fission track ages in the same intrusions, may represent the time lag required for complete relaxation of the perturbations of the isotherms in the geothermal field imposed by intrusion of magmatic bodies, instead of exhumation-related cooling. However, the above age-elevation relationship favors the latter.

The cooling histories of intrusive bodies depend on their volume, shape, and level of emplacement. According to numerical simulations, ascent and emplacement of granitic intrusions in the upper crust typically occurs in less than 1 m.yrs. (Kukowski and Neugebauer 1990; Cathles *et al*., 1997; Adriasola *et al*., 2006). Such rapid cooling is inferred for the Cruz de Piedra intrusion, which is an unaltered quartz monzonite stock that crops out close to the continental watershed at 3,790 m of altitude (near the Chilean-Argentinean border; Fig. 2). We have obtained an apatite fission track age of 6.1±0.6 Ma (mean track length: 14.95±0.10 μm), and an identical zircon fission track age of 6.2±0.4 Ma for this stock (ETP-14; Table 4). Previously, Kurtz *et al*. (1997) reported a biotite $^{40}Ar/^{39}Ar$ plateau age of 5.5±0.1 Ma for the same sample (ETP-14), which is equivalent to these fission track ages (within $\pm 2\sigma$ error limits). Considering the differing temperature ranges of the apatite and zircon fission track annealing zones, and the closure temperature of biotite for the K-Ar system, the similar ages imply very rapid *in situ* post-magmatic cooling, as shown by the temperature-time path below 350°C, which is consistent with high cooling rates (>200°C/m.yrs; Fig. 5).

At shallow levels in the upper crust (~5 km), heat transfer from a magma chamber is likely to occur through convection of hydrothermal fluids. Depending on the permeability of the wallrock, the anomalous heat flow affects the shape and distribution of the geothermal gradients in their surroundings, lifting the isotherms in the area above

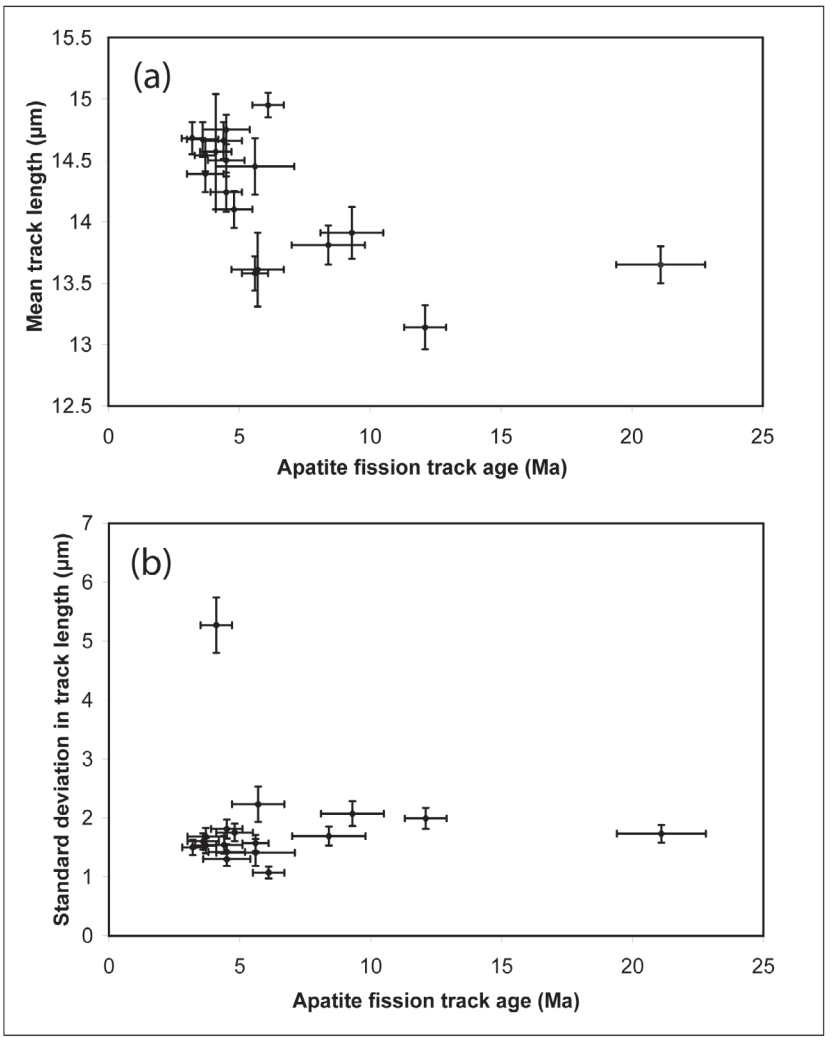

FIG. 3. Relationship between the apatite fission track age to **a.** mean track length, and **b.** standard deviation in track length. Relationship is shown for all apatite samples which yielded adequate track length data. Long track lengths (>14 µm) and small standard deviations (<1.5 µm) define a distinctive cooling episode between ~6 and 3 Ma, during which intrusive rocks from the western slope of the high Andean Cordillera cooled through the ~125-60ºC temperature range (apatite partial annealing zone).

the chamber towards the surface of the Earth (*e.g.*, Adriasola *et al*., 2006). This situation is recognized at the Río Blanco porphyry copper deposit, which was formed by hydrothermal fluids in association with an epizonal, multistage intrusive complex from 6.3±0.1 Ma to 4.3±0.1 Ma according to U-Pb, $^{40}Ar/^{39}Ar$, K-Ar and Re-Os ages (Deckart *et al*., 2005). Our apatite fission track ages for underground samples of the hydrothermally altered/mineralized Río Blanco granodiorite are 3.7±0.4 and 3.2±0.4 Ma (Tables 2 and 4). In addition, apatite (U-Th)/He ages of 3.5±0.1 and 2.4±0.1 Ma were reported by McInnes *et al.* (2005) for the quartz monzonite and Don Luis porphyries of the Río Blanco orebody. These data attest to exceedingly rapid cooling of the hydrothermal system after cessation of the igneous pulses; *i.e.*, within ~1 m.yrs. for cooling through the temperature range of the apatite partial annealing zone (~125°-60°C) and within ~2 m.yrs. through the temperature range of the apatite He partial retention zone (~85°-40°C; Wolf *et al*., 1998).

A similar evolution is inferred for the El Teniente porphyry copper deposit, which according to combined U-Pb, $^{40}Ar/^{39}Ar$, K-Ar and Re-Os ages formed from 6.5±0.1 Ma to 4.3±0.1 Ma (Maksaev *et al*., 2004), and a post-ore hornblende-rich andesitic dike intruded at 3.85±0.18 Ma marks the end of igneous activity within the orebody (Maksaev *et al*., 2004). An apatite fission track age of 4.2±2.8 Ma (Maksaev *et al*., 2004), and apatite (U-Th)/He ages from 3.4 to 2.7 Ma for the dacite porphyry of El Teniente (McInnes *et al*., 2005), provide evidence for fast

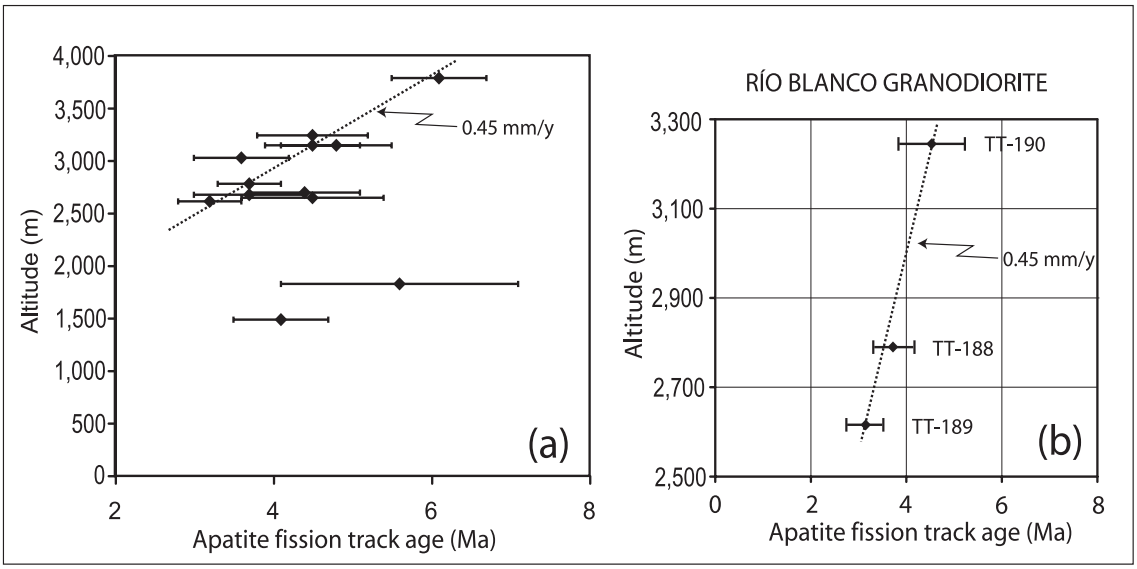

FIG. 4. Relationship between apatite fission track age to elevation for: **a.** all samples with long mean track lengths (>14.0 μm) and small standard deviations (<1.8 μm) (Units: Río Blanco, Jeria, Extravío, Alfalfalito, Cruz de Piedra, Río Pangal, Estero Crucero, Rosario de Rengo, and Río Cortaderal) and **b.** subset of three samples from drill cores into the Río Blanco granodiorite. As a reference, dashed lines corresponding to hypothetical exhumation rates of 0.45 mm/y are shown on both figures.

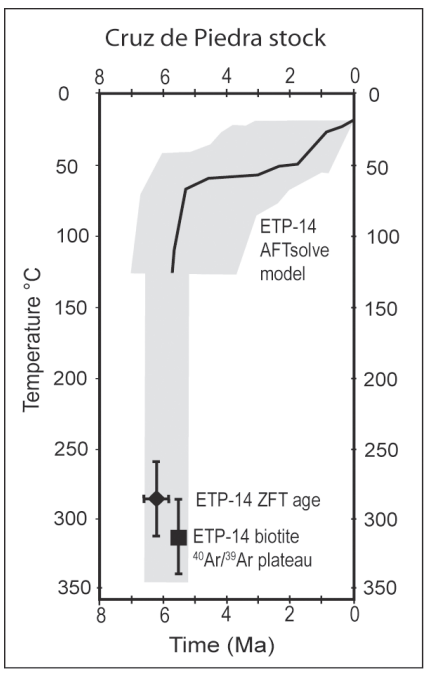

FIG. 5. Time-temperature path for sample ETP-14 from the Cruz de Piedra stock, combining the biotite $^{40}Ar/^{39}Ar$ plateau age (Kurtz *et al*., 1997), the respective zircon fission track age, and the AFTsolve model based on apatite fission track data (best fit line and shading of acceptable fit solutions are shown in the AFTsolve model).

cooling of this giant porphyry system after the end of the igneous intrusions.

Temperature-time paths were constructed combining previous geochronological data, new zircon fission track ages, and inverse modelling of apatite fission track data using the AFTsolve multi-kinetic program of Ketcham *et al*. (2000) for the Río Blanco, Extravío, Alfalfalito, Río Pangal, Estero Crucero, Santa Rosa de Rengo, and Nacientes Río Cortaderal plutons (Figs. 6, 7 and 8). The fission track ages of these plutons range from 5.6±1.5 to 3.2±0.4 Ma, and are 2 to 7 m.yrs. younger than their respective zircon fission track and $^{40}Ar/^{39}Ar$ ages (Table 4). Furthermore, their apatite grains have long mean fission track lengths (>14.0 μm; Fig. 2) and narrow track length distributions (standard deviations <1.5 μm), consistent with rapid cooling through the temperature range of the apatite partial annealing zone (~125-60°C). In general, their temperature-time paths are consistent with rapid post-magmatic cooling, with delays of 2 to 7 m.yrs. for cooling through the temperature range of the apatite partial annealing zone (~125-60°C). Although extended igneous-linked cooling cannot be completely discarded, the relatively long time-lag for cooling below ~125°C and the modelled cooling histories are

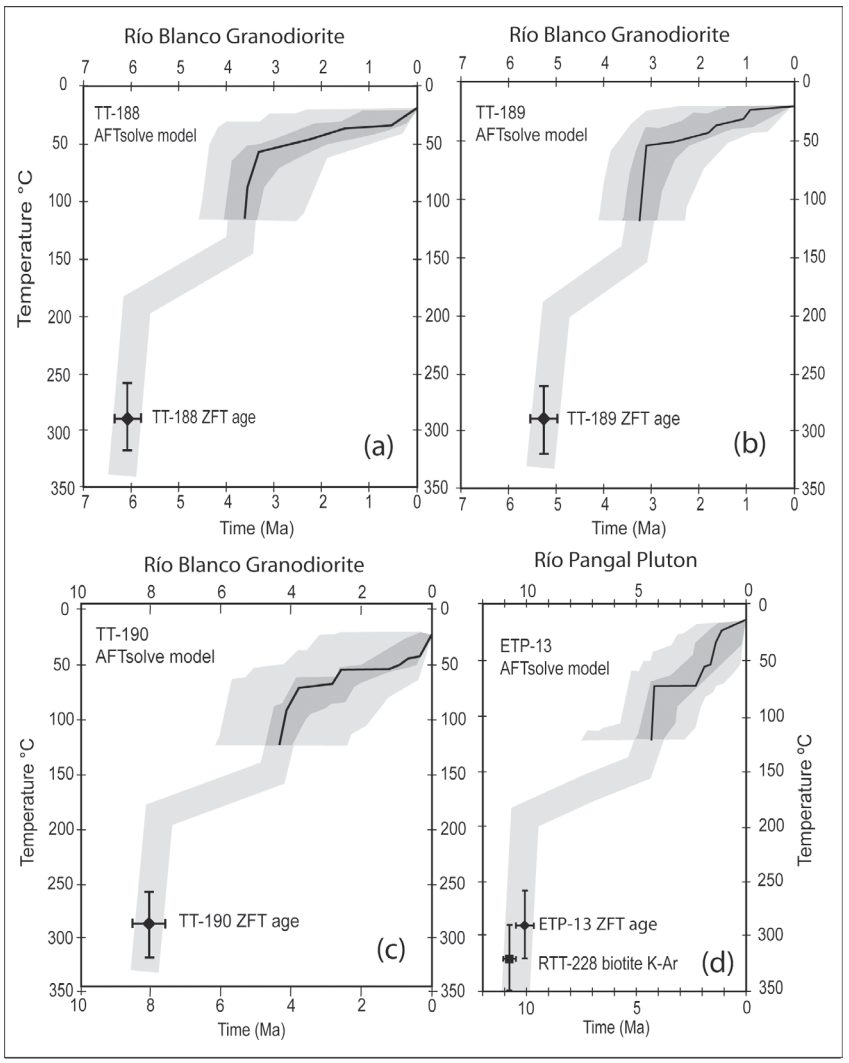

FIG. 6. Time-temperature paths, combining zircon fission track ages with the model thermal history for apatite samples, for: **a.** sample TT-188; **b.** sample TT-189, and **c.** sample TT-190 from drill core samples of the Río Blanco granodiorite; and **d.** sample ETP-13 from the Río Pangal pluton (AFTsolve best fit line and shading of good and acceptable fit solutions are shown).

strongly suggestive of a distinct cooling event at ~6 to 3 Ma, probably related to subsequent, enhanced exhumation of these intrusive bodies.

The exhumation of the Miocene plutons along the western slope of the Principal Andean Cordillera (33-35°S) from ~6 to 3 Ma may well be a consequence of enhanced erosion related to increased relief, due to crustal shortening and surface uplift related to the Pliocene Diaguita compressive tectonism of Salfity *et al*. (1984). It coincides with the time of the southward migration of the location of the collision of the Juan Fernández Ridge against the South American margin at these latitudes accompanied by the progressive onset of flat subduction from north to south (Yáñez *et al*., 2002). It probably represents part of a period of accelerated denudation as proposed by Skewes and Holmgren (1993), and overlap in time with documented Pliocene massive landslides along the western slope of the Principal Andean Cordillera (Encinas *et al*., 2006; and references therein). In fact, rapid unroofing of the Río Blanco porphyry Cu-Mo orebody took place before being covered by rhyodacitic tuff deposits of the La Copa complex dated by K-Ar from 4.9±0.2 to 4.0±0.2 Ma (Vergara and Drake, 1978; Serrano *et al*., 1996; Deckart *et al*., 2005).

Supplementary data comes from the geomorphologic analysis of Farías *et al*. (2008), who inferred the onset of high and rapid surface uplift in the Andes of Central Chile (33-35°) between 10.5 and 4.6 Ma, and the thermochronological study of Spikings *et al*. (2008) that estimated the onset

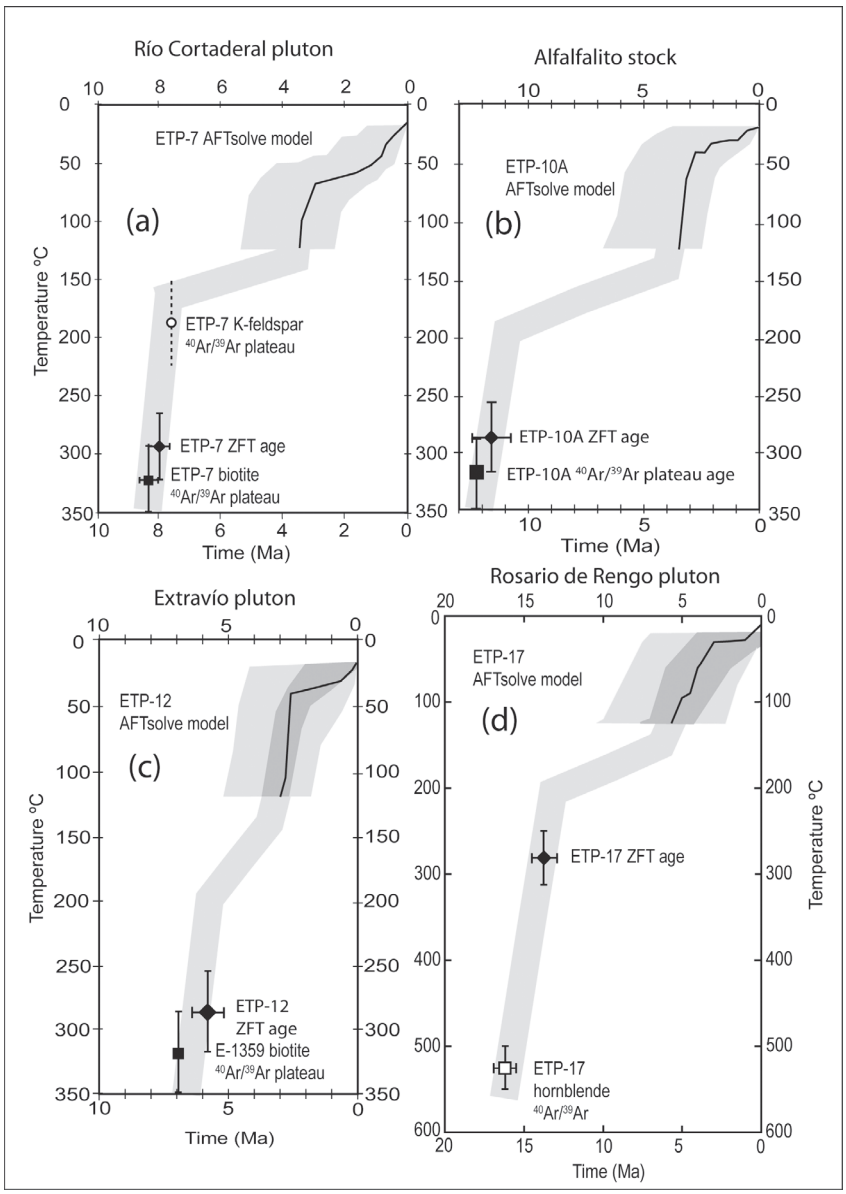

FIG. 7. Time-temperature path combining the $^{40}Ar/^{39}Ar$ ages after Kurtz *et al*. (1997), the respective zircon fission track ages, and the AFTsolve model based on apatite fission track data for: **a.** sample ETP-7 from the Río Cortaderal pluton; **b.** sample ETP-10A from the Alfalfalito stock; **c.** sample ETP-12 from the Extravío pluton; and **d.** sample ETP-17 from the Rosario de Rengo pluton (AFTsolve model best fit line and shading of good and acceptable fit solutions are shown).

of exhumation at about 7.5 Ma for the segment of the Principal Andean Cordillera in Chile located immediately south between 35-38°S, based on $^{40}Ar/^{39}Ar$, apatite fission track and zircon and apatite (U-Th)/He data. Spikings *et al*. (2008) also showed that exhumation between 35-38°S occurred at progressively earlier times northward, to the region that is at present above the flat slab segment, which hosts the Juan Fernández Ridge. This fits well with our apatite fission track data between about 6 and 3 Ma representing the youngest exhumation between 33-35°S.

Previous independent geological evidence of the late Miocene-Pliocene uplift in the Andes of Central Chile, lead Skewes and Holmgren (1993) to postulate that the associated rapid exhumation of active plutonic systems during this regime triggered exsolution of magmatic fluids with copper, which produced hydrothermal brecciation, and stockwork mineralization of the supergiant Río Blanco-Los Bronces and El Teniente porphyry copper deposits during the late Miocene and Pliocene. Actually, according to our data these epizonal intrusions cooled and consequently crystallized too fast for

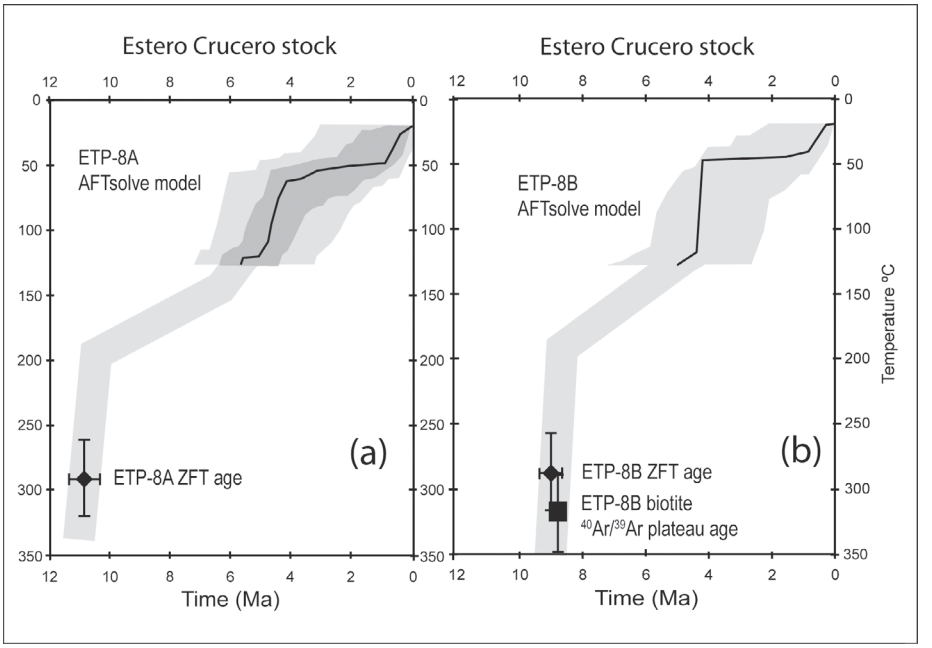

FIG. 8. Time-temperature, combining a biotite $^{40}Ar/^{39}Ar$ plateau age after Kurtz *et al*. (1997), the respective zircon fission track ages, and the AFTsolve model based on apatite fission track data path, for: **a.** sample ETP-8A and **b.** sample ETP-8B from the Estero Crucero stock (AFTsolve model best fit line and shading of good and accept-able fit solutions are shown).

being significantly affected by pressure release from long-lasting, steady exhumation. Then again, exhumation does not progress at constant rates, and our fission track data strongly suggest accelerated exhumation cooling between ~6 and 3 Ma, coinciding with mass wasting of the volcanic cover of porphyry deposits (*e.g.*, Godoy *et al*., 1994; Encinas *et al*., 2006). Thus mineralizing processes, brecciation, and formation of diatreme vents at the Río Blanco-Los Bronces and El Teniente porphyry copper systems (*e.g.*, Sillitoe, 1985), probably was related to the gravitational sliding of their volcanic roof. Actually, overpressure of hydrothermal fluids may have been fundamental to trigger the landslides of the volcanic cover on top of the porphyry systems similarly to the model of Reid (2004), and sudden unroofing by gravitational sliding during the magmatic-hydrothermal evolution of these deposits may have destabilized the deeper magma chambers and may have influenced magma degassing and the development of shallow, richly-mineralized, late hydrothermal breccias and explosive diatreme vents within these world class Cu-Mo deposits.

6. Conclusions

Fission track thermochronology of Miocene plutons of the Principal Andean Cordillera of central Chile revealed that most intrusions yield younger apatite fission track ages relative to their $^{40}Ar/^{39}Ar$ ages, and zircon fission track ages, respectively. The long track lengths (>14 μm) and small standard deviations (<1.5 μm) of the apatite samples from most of these plutons and their age data define a distinctive episode of enhanced cooling between about 6 and 3 Ma. During this period the dated rocks of the western slope of the Principal Andean Cordillera cooled rapidly through the temperature range of the apatite partial annealing zone (~125-60°C), consistent with accelerated exhumation rates throughout the latest Miocene and early Pliocene as a consequence of surface uplift associated with the Diaguita compressive tectonism. The timing coincides with the southward migration of the locus of the collision of the Juan Fernández Ridge against the South American margin at these latitudes, accompanied by the progressive onset of flat subduction from

north to south. As a consequence, it also appears that there was a progressively older onset of exhumation southwards along the Principal Andean Cordillera as inferred from our recently published thermochronological data.

The 6 to 3 Ma period coincides with the rapid unroofing of some of the largest porphyry Cu-Mo deposits in the world (El Teniente, Río Blanco-Los Bronces) at the time of their intrusion-related mineralization processes and also with mass wasting processes on the largely volcanic western slope of the Principal Andean Cordillera in central Chile. Massive landslides during the Pliocene may have had an effect on magma degassing and the development of shallow, richly-mineralized, late hydrothermal breccias and explosive diatremes within these world class Cu-Mo deposits.

The thermochronologic zircon fission track data are consistent with *in situ* post-magmatic rapid cooling of the intrusions, and a maximum of about 8 km of Neogene exhumation of the dated plutons. The relatively limited exhumation contributed to the preservation of the shallow late Miocene-early Pliocene Cu-Mo deposits and Neogene volcanic succession along the western slope of the Principal Andean Cordillera in central Chile.

Acknowledgments

This study benefited from the Program for Incentive of International Cooperation 7000932 of CONICYT, Chile, and Fondecyt Grant 1000932. The analytical contribution of Dr. P.B. O'Sullivan of Apatite to Zircon, Inc., USA, and Dr. A.M. (Sandy) Grist of Dalhousie University, Canada, is sincerely appreciated. Special thanks to P. Zúñiga and A. Arévalo for authorizing the analyses of the samples collected during a previous regional project in the region ('Proyecto Geodinámico El Teniente') of El Teniente Division, CODELCO, Chile. Comments provided by the reviewers S.N. Thomson, S.M. Kay and L. Barbero helped to improve and clarify the manuscript. This is a contribution to the Anillo ACT-18 project: 'Tectonomagmatic control of Giant Ore Deposits in the subduction factory of the High Chilean Andes between 32º-36ºS: A multidisciplinary Approach' (TECMA-GOD-MULTI).

References

Adriasola, A.C.; Thomson, S.N.; Brix, M.R.; Hervé, F.; Stöckhert, B. 2006. Postmagmatic cooling and late Cenozoic denudation of the North Patagonian Batholith in the Los Lagos region of Chile, 41°-42°15'S. International Journal of Earth Sciences 95: 504-528.

Adriasola, A.C.; Stöckhert, B. 2008. Cooling histories and deformation of plutonic rocks along the Liquiñe-Ofqui Fault Zone, Southern Chile (41°-42°15'S). Revista Geológica de Chile 35 (1): 39-61.

Aguirre, L. 1960. Geología de los Andes de Chile Central, Provincia de Aconcagua. Instituto de Investigaciones Geológicas, Boletín 9: 70 p.

Bernet, M.; Garver, J.I. 2005. Fission-track analysis of detrital zircon. Reviews in Mineralogy and Geochemistry 58: 205-238.

Bernet, M.; Brandon, M.T.; Garver, J.I.; Reiners, P.W.; Fitzgerald, P.G. 2002. Determining the zircon fission-track closure temperature. Geological Society of America, Abstracts with Programs 34: 18 p.

Brandon, M.T.; Roden-Tice, M.K.; Garver, J.I. 1998. Late Cenozoic exhumation of the Cascadia accretionary wedge in the Olympic mountains, northwest Washington State. Geological Society of America Bulletin 110: 985-1009.

Cahill, T.; Isacks, B.L. 1992. Seismicity and shape of the subducted Nazca plate. Journal of Geophysical Research 97: 17503-17529.

Cannell, J.; Cooke, D.R.; Walshe, J.L.; Stein, H. 2005. Geology, Mineralization, Alteration, and Structural Evolution of the El Teniente Porphyry Cu-Mo Deposit. Economic Geology 100: 979-1003.

Carlson, W.D.; Donelick, R.A.; Ketcham, R.A. 1999. Variability of apatite fission track annealing kinetics: I Experimental results. American Mineralogist 34: 1213-1223.

Cathles, L.M.; Erendi, A.H.J.; Thayer, J.B.; Barrie, T. 1997. How long can a hydrothermal system be sustained by a single intrusion event? Economic Geology 92: 766-771.

Charrier, R.; Baeza, O.; Elgueta, S.; Flynn, J.J.; Gans, P.; Kay, S.M.; Muñoz, N.; Wyss, A.R.; Zurita, E. 2002. Evidence for Cenozoic extensional basin development and tectonic inversion south of the flat-slab segment, southern Central Andes, Chile (33º-36ºS.L.). Journal of South American Earth Sciences 15: 117-139.

Charrier, R.; Bustamante, M.; Comte, D.; Elgueta, S.; Flynn, J.J.; Iturra, N.; Muñoz, N.; Pardo, M.; Thiele, R.; Wyss, A.R. 2005. The Abanico Extensional Basin: regional extension, chronology of tectonic inversion and relation to shallow seismic activity and Andean uplift. Neues Jahrbuch für Geologie und Paläontologie, Abhandlungen 236: 43-77.

Charrier, R.; Pinto, L.; Rodríguez, M.P. 2007. Tectonostatigraphic evolution of the Andean Orogen in Chile. *In* The Geology of Chile (Moreno, T.; Gibbons, W.; editors). The Geological Society: 21-114. London.

Deckart, K.; Clark, A.H.; Aguilar, C.; Vargas, R.; Bertens, A.; Mortensen, J.K.; Fanning, M. 2005. Magmatic and hydrothermal geochronology of the giant Río Blanco porphyry copper deposit, central Chile: Implications of an integrated U-Pb and $^{40}Ar/^{39}Ar$ database. Economic Geology 100: 905-934.

Deckart, K.; Clark, A.H.; Cuadra, P.; Bertens, A. 2006. Diachronous and protracted magmatic and hydrothermal activity in the Río Blanco porphyry copper-molybdenum deposit cluster, central Chile: new SHRIMP U-Pb, Re-Os and $^{40}Ar/^{39}Ar$ age data. *In* Congreso Geológico Chileno, No. 11, Actas 2: 231-234. Antofagasta.

Dodson, M.H. 1973. Closure temperature in cooling geochronological and petrological systems. Contributions to Mineralogy and Petrology 40: 259-274.

Donelick, R.A.; Ketcham, R.A.; Carlson, W.D. 1999. Variability of apatite fission track annealing kinetics II: Crystallographic orientation effects. American Mineralogist 84: 301-307.

Encinas, A.; Maksaev, V.; Pinto, L.; Le Roux, J.P.; Munizaga, F.; Zentilli, M. 2006. Pliocene lahar deposits in the Coastal Cordillera of central Chile, as related to uplift, avalanche deposits and porphyry copper systems in the Main Andean Cordillera. Journal of South American Earth Sciences 20: 369-381.

Farías, M.; Charrier, R.; Carretier, S.; Martinod, J.; Fock, A.; Campbell, D.; Cáceres, J.; Comte, D. 2008. Late Miocene high and rapid surface uplift and its erosional response in the Andes of central Chile (33°-35°S). Tectonics 27: TC1005, doi:10.1029/2006TC002046.

Gallagher, K.; Brown, R.; Johnson, C. 1998. Fission track analysis and its applications to geological problems. Annual Review of Earth and Planetary Sciences 26: 519-572.

Giambiagi, L.B.; Tunik, K.; Ghiglione, M. 2001. Cenozoic tectonic evolution of the Alto Tunuyán foreland basin above the transition zone between the flat and normal subduction segment (33°30'-34°00'S), western Argentina. Journal of South American Earth Sciences 14: 707-724.

Giese, P. 1994. Geothermal structure of the Central Andean crust-Implication for heat transport and rheology. *In* Tectonics of the Southern Central Andes: Structure and evolution of an active continental margin (Reutter, K.-J.; Scheuber, E.; Wigger, P.J.; editors). Springer-Verlag: 69-76. Berlin.

Gilbert, H.; Beck, S.; Zandt, G. 2006. Lithospheric and upper mantle structure of central Chile and Argentina. Geophysical Journal International 165: 383-398.

Gleadow, A.J.W. 1981. Fission track dating methods: what are the real alternatives? Nuclear Tracks and Radiation Measurements 5: 3-14.

Gleadow, A.J.W.; Duddy I.R.; Green, P.F.; Heggarty, K.A. 1986. Fission track lengths in the apatite annealing zone and the interpretation of mixed ages. Earth and Planetary Science Letters 78: 245-254.

Godoy, E.; Lara, L.; Burmester, R. 1994. El 'Lahar' Cuaternario de Colón-Coya: Una avalancha de detritos pliocena. *In* Congreso Geológico Chileno, No. 7, Actas 1: 305-309. Concepción.

Godoy, E.; Yáñez, G.; Vera, E. 1999. Inversion of an Oligocene volcano-tectonic basin and uplifting of its superimposed Miocene magmatic arc in the Chilean Central Andes: first seismic and gravity evidences. Tectonophysics 306: 217-236.

González-Bonorino, G.; Kraemer, P.; Re, G. 2001. Andean Cenozoic foreland basins: a review. Journal of South American Earth Sciences 14: 651-654.

Green, P.F. 1981. A new look to statistics in fission track dating. Nuclear Tracks and Radiation Measurements 5: 77-86.

Green, P.F.; Duddy, I.R.; Gleadow, A.J.W.; Tingate, P.R.; Laslett, G.M. 1986. Thermal annealing of fission tracks in apatite 1: A qualitative description. Chemical Geology 59: 237-253.

Green, P.F.; Duddy, I.R.; Laslett, G.M.; Hegarty, K.A.; Gleadow, A.J.W.; Lovering, J.F. 1989. Thermal annealing of fission tracks in apatite 4: Quantitative modelling techniques and extension to geological time scales. Chemical Geology 79: 155-182.

Hamza, V.M.; Muñoz, M. 1996. Heat flow map of South America. Geothermics 25: 599-646.

Harrison, T.M.; Duncan, I.; McDougall, I. 1985. Diffusion of ^{40}Ar in biotite: temperature, pressure and compositional effects. Geochimica et Cosmochimica, Acta 49: 2461-2468.

Hurford, A.J. 1986. Cooling and uplift pattern in the Lepontine Alps, South Central Switzerland and an age of vertical movement on the Insubric fault line. Contributions to Mineralogy and Petrology 92: 413-427.

Hurford, A.J.; Green, P.F. 1983. The zeta age calibration of fission track dating. Isotope Geoscience 1: 285-317.

Kay, S.M.; Mpodozis, C. 2002. Magmatism as a probe to the Neogene shallowing of the Nazca plate beneath the modern Chilean flat-slab. Journal of South American Earth Sciences 15: 39-57.

Kay, S.M.; Mpodozis, C.; Coira, B. 1999. Neogene magmatism, tectonism and mineral deposits of the Central Andes (22°-33°S Latitude). *In* Geology and Ore Deposits of the Central Andes (Skinner, B.J.; editor). Society of Economic Geologists, Special Publication 7: 27-59.

Kay, S.M.; Godoy, E.; Kurtz, A. 2005. Episodic arc migration, crustal thickening, subduction erosion, and magmatism in the south-central Andes. Geological Society of America Bulletin 117: 67-88.

Ketcham, R.A.; Donelick, R.A.; Carlson, W.D. 1999. Variability of apatite fission track annealing kinetics III: Extrapolations to geological time scales. American Mineralogist 84: 1235-1255.

Ketcham, R.A.; Donelick, R.A.; Donelick, M.B. 2000. AFTsolve: A program for multi-kinetic modelling of apatite fission-track data. Geological Materials Research 2: 1-32.

Klohn, C. 1960. Geología de la Cordillera de los Andes de Chile Central. Provincias de Santiago, Colchagua y Curicó. Instituto de Investigaciones Geológicas, Boletín 8: 95 p.

Kukowski, N.; Neugebauer, H.J. 1990. On the ascent and

emplacement of granitoid magma bodies-dynamic-thermal numerical models. Geologische Rundschau 79: 227-239.

Kurtz, A.C.; Kay, S.M.; Charrier, R.; Farrar, E. 1997. Geochronology of Miocene plutons and exhumation history of the El Teniente region, Central Chile (34º-35ºS). Revista Geológica de Chile 24 (1): 75-90.

Laslett, G.M.; Green, P.F.; Duddy, I.R.; Gleadow, A.J.W. 1987. Thermal annealing of fission tracks in apatite 2: A quantitative analysis. Chemical Geology 65: 1-15.

Maksaev, V.; Munizaga, F.; McWilliams, M.; Fanning, M.; Mathur, R.; Ruiz, J.; Zentilli, M. 2004. New chronology for El Teniente, Chilean Andes, from U/Pb, $^{40}Ar/^{39}Ar$, Re-Os and fission track dating: Implications for the evolution of a supergiant porphyry Cu-Mo deposit. *In* Andean Metallogeny: New Discoveries, Concepts and Updates (Sillitoe, R.H.; Perelló, J.; Vidal, C.E.; editors). Society of Economic Geologists, Special Publication 11: 15-54.

Marangunic, C.; Moreno, H.; Varela, J. 1979. Observaciones sobre los depósitos de relleno de la Depresión Longitudinal de Chile entre los ríos Tinguiririca y Maule. *In* Congreso Geológico Chileno, No. 2, Actas 11: 129-139. Arica.

McDougall, I.; Harrison, T.M. 1999. Geochronology and Thermochronology by the $^{40}Ar/^{39}Ar$ Method. Oxford University Press: 269 p. New York.

McInnes, B.I.A.; Evans, N.J.; Fu, F.Q.; Garwin, S.; Belousova, E.; Griffin, W.L.; Bertens, A.; Sukarna, D.; Permanadewi, S.; Andrew, R.L.; Deckart, K. 2005. Thermal history analysis of selected Chilean, Indonesian, and Iranian porphyry Cu-Mo-Au deposits. *In* Super Porphyry Copper and Gold Deposits: A Global Perspective (Porter, T.M.; editor). Porter Geoconsultancy Publishing, de Adelaide, Australia: 27-42.

Muñoz, M. 1999. Tectonophysics of the Andes region: relationships with heat flow and the thermal structure. *In* International Symposium on Andean Geodynamics, No. 4, Abstracts: 532-534. Göttingen, Germany.

Nyström, J.; Vergara, M.; Morata, D.; Levi, B. 2003. Tertiary volcanism in central Chile (33°15'-33°45'S): the passage toward an Andean setting with time. Geological Society of America Bulletin 115: 1523-1537.

Pardo, M.; Comte, D.; Monfret, T. 2002. Seismotectonic and stress distribution in the central Chile subduction zone. Journal of South American Earth Sciences 15: 11-22.

Ramos, V.; Cegarra, M.; Cristallini, E. 1996. Cenozoic tectonics of the High Andes of west-central Argentina (30°-36°S latitude). Tectonophysics 259: 185-200.

Reid, M.E. 2004. Massive collapse of volcano edifices triggered by hydrothermal pressurization. Geology 32: 373-376.

Reiners, P.W.; Brandon, M.T. 2006. Using thermochronology to understand orogenic erosion. Annual Review of Earth and Planetary Sciences 34: 419-466.

Salfity, J.A.; Gorustovich, S.A.; Moya, M.C.; Amengual, R. 1984. Marco tectónico de la sedimentación y efusividad cenozoicas en la Puna argentina. *In* Congreso Geológico Argentino, No. 9, Actas 1: 539-554. Buenos Aires.

Seipold, U. 1998. Temperature dependence of thermal transport properties of crystalline rocks-A general law. Tectonophysics 91: 161-171.

Sellés, D.; Gana P. 2001. Geología del area Talagante-San Francisco de Mostazal: Regiones Metropolitana y del Libertador General Bernardo O'Higgins. Servicio Nacional de Geología y Minería, Carta Geológica de Chile, Serie Geología Básica 74: 30 p., escala 1:100.000.

SERNAGEOMIN. 2002. Mapa Geológico de Chile. Servicio Nacional de Geología y Minería, Carta Geológica de Chile, Serie Geología Básica 75, escala 1:1.000.000.

Serrano, L.; Vargas, R.; Stambuk, V.; Aguilar, C.; Galeb, M.; Holgrem, C.; Contreras, A.; Godoy, S.; Vela, I.; Skewes, M.A.; Stern, C.R. 1996. The late Miocene Río Blanco-Los Bronces copper deposit, central Chilean Andes. *In* Andean Copper Deposits: New Discoveries, Mineralization, Styles and Metallogeny (Camus, F.; Sillitoe, R.H.; Petersen, R.; editors). Society of Economic Geologists, Special Publication 5:119-130.

Sillitoe, R.H. 1985. Ore-related breccias in volcanoplutonic arcs. Economic Geology 80: 1467-1514.

Sillitoe, R.H.; Perelló, J. 2005. Andean copper province: tectonomagmatic settings, deposit types, metallogeny, exploration, and discovery. *In* Economic Geology One Hundredth Anniversary (Hedenquist, J.W.; Thompson, J.F.H.; Goldfarb, R.; Richards, J.; editors). Society of Economic Geologists 1905: 845-890.

Skewes, M.A.; Holmgren, C. 1993. Solevantamiento andino, erosión y emplazamiento de brechas mineralizadas en el depósito de cobre porfídico Los Bronces, Chile central (33°S), aplicación de geotermometría de inclusiones fluidas. Revista Geológica de Chile 20 (1): 71-84.

Skewes, M.A.; Stern, C.R. 1994. Tectonic trigger for the formation of Late Miocene Cu-rich megabreccias in the Andes of central Chile. Geology 22: 551-554.

Skewes, M.A.; Arévalo, A.; Floody, R.; Zúñiga, P.; Stern, C.R. 2002. The giant El Teniente breccia deposit: hypogene copper distribution and emplacement. *In* Integrated methods for discovery: global exploration in the twenty-first century (Goldfarb, R.J.; Nielsen, R.L.; editors). Society of Economic Geologists, Special Publication 9: 299-332.

Spikings, R.A.; Winklerb, W.; Hughesc, R.A.; Handler, R. 2005. Thermochronology of allochthonous terranes in Ecuador: Unravelling the accretionary and post-accretionary history of the Northern Andes. Tectonophysics 399: 195-220.

Spikings, R.; Dungan, M.; Foeken, J.; Carter, A.; Page, L.;

Stuart, F. 2008. Tectonic response of the central Chilean margin (35-38°S) to the collision and subduction of heterogeneous oceanic crust: a thermochronological study. Journal of the Geological Society of London 165: 941-953.

Steinmann, G. 1929. Geologie von Perú. Carl Winters Universitätsbuchhandlung, Heidelberg: 448 p.

Stern, C.R.; Skewes, M.A. 2005. Origin of giant Miocene and Pliocene Cu-Mo deposits in central Chile: role of ridge subduction, decreased subduction angle, subduction erosion, crustal thickening, and long-lived, batholith-size, open system magma chambers. *In* Super Porphyry Copper and Gold Deposits, A Global Perspective (Porter, T.M.; editor). Porter Geoconsultancy Publishing, de Adelaide, Australia 1: 65-82.

Tagami, T. 2005. Zircon fission-track thermochronology and applications to fault studies. Reviews in Mineralogy and Geochemistry 58: 95-122.

Tagami, T.; Shimada, C. 1996. Natural long-term annealing of the zircon fission-track system around a granitic pluton. Journal of Geophysical Research 101: 8245-8255.

Thiele, R. 1980. Hoja Santiago, Región Metropolitana. Servicio Nacional de Geología y Minería, Carta Geológica de Chile 29: 21 p., escala 1:250.000.

Thomson, S.N.; Hervé, F.; Stöckhert, B. 2001. The Mesozoic-Cenozoic denudation history of the Patagonian Andes (southern Chile) and its correlation to different subduction processes. Tectonics 20: 693-711.

Vergara, M.; Drake, R. 1978. Edades potasio-argón y su implicancia en la geología regional de Chile central. Comunicaciones 23: 1-11.

Wolf, R.A.; Farley, K.A.; Kass, D.M. 1998. Modelling of the temperature sensitivity of the apatite (U-Th)/He thermochronometer. Chemical Geology 148: 105-114.

Yáñez, G.; Ranero, C.R.; von Huene, R.; Díaz, J. 2001. Magnetic anomaly interpretation across the southern central Andes (32°-34°S): the role of the Juan Fernández Ridge in the late Tertiary evolution of the margin. Journal of Geophysical Research 106: 6325-6345.

Yáñez, G.; Cembrano, J.; Pardo, M.; Ranero, C.R.; Selles, D. 2002. The Challenger-Juan Fernández-Maipo major tectonic transition of the Nazca-Andean subduction system at 33-34°S: geodynamic evidence and implications. Journal of South American Earth Sciences 15: 23-38.

Manuscript received: September 09, 2008; revised/accepted: December 22, 2008.